Prognostics of Power MOSFETs under Thermal Stress Accelerated Aging using Data-Driven and Model-Based Methodologies

José R. Celaya [1], Abhinav Saxena [2], Sankalita Saha [3] and Kai F. Goebel [4]

[1,2] SGT Inc., NASA Ames Research Center, Prognostics Center of Excellence, Moffett Field, CA, 94035, USA
Jose.R.Celaya@nasa.gov
Abhinav.Saxena@nasa.gov

[3] MCT, NASA Ames Research Center, Prognostics Center of Excellence, Moffett Field, CA, 94035, USA
Sankalita.Saha@nasa.gov

[4] NASA Ames Research Center, Prognostics Center of Excellence, Moffett Field, CA, 94035, USA
Kai.Goebel@nasa.gov

ABSTRACT

An approach for predicting remaining useful life of power MOSFETs (metal oxide field effect transistor) devices has been developed. Power MOSFETs are semiconductor switching devices that are instrumental in electronics equipment such as those used in operation and control of modern aircraft and spacecraft. The MOSFETs examined here were aged under thermal overstress in a controlled experiment and continuous performance degradation data were collected from the accelerated aging experiment. Die-attach degradation was determined to be the primary failure mode. The collected run-to-failure data were analyzed and it was revealed that ON-state resistance increased as die-attach degraded under high thermal stresses. Results from finite element simulation analysis support the observations from the experimental data. Data-driven and model based prognostics algorithms were investigated where ON-state resistance was used as the primary precursor of failure feature. A *Gaussian process regression* algorithm was explored as an example for a data-driven technique and an *extended Kalman filter* and a *particle filter* were used as examples for model-based techniques. Both methods were able to provide valid results. Prognostic performance metrics were employed to evaluate and compare the algorithms.

1. INTRODUCTION

Power semiconductor devices such as MOSFETs (Metal Oxide Field Effect Transistors) and IGBTs (Insulated Gate Bipolar Transistors) are essential components of electronic and electrical subsystems in on-board autonomous functions for vehicle controls, communications, navigation, and radar systems. Until very recently it was common wisdom that electronic devices fail instantly without any prior indication of failure. Therefore, current maintenance schedules are usually based on reliability data available from the manufacturer. This approach works well in aggregate on a large number of components, but, owing to the statistics, failures on individual components are not necessarily averted. For mission critical systems it is extremely important to avoid such failures. This calls for condition based prognostic health management methods. The science of prognostics is based on the analysis of failure modes, detection of early signs of wear and aging, and fault conditions. Predictions are made *in-situ* on individual in-service components. The signs of early wear are then correlated with a damage propagation model and suitable prediction algorithms to arrive at a remaining useful life (RUL) estimate.

To carry out prognostics on electronic components it is essential to understand the failure modes, their effects, and the physics of fault propagation. This requires analysis of run-to-failure data. Since more often than not current systems are not adequately instrumented to provide necessary information from electronic components to build health management algorithms, dedicated experiments are needed to fill that gap. In particular, accelerated aging allows collecting run-to-failure data in a manageable timeframe. The prognostic technique for a power MOSFET presented in this paper is based on accelerated aging of MOSFET IRF520Npbf (which comes in a TO-220 package). The aging methodology utilizes thermal and power cycling and was validated with tests using 100V power MOSFET devices. The major failure mechanism for

the stress conditions is die-attachment degradation, typical for discrete devices with lead-free solder die attachment. It has been determined in these experiments that die-attach degradation results in an increase in ON-state resistance due to its dependence on junction temperature. Increasing resistance, thus, can be used as a precursor of failure for the die-attach failure mechanism under thermal stress. Data collected from these experiments were augmented by a finite element analysis simulation based on a two-transistor model. The features based on normalized ON-resistance were computed from *in-situ* measurements of the electro-thermal response. A Gaussian process regression (GPR) framework to predict time to failure was used as a data-driven prognostics technique. The extended Kalman filter (EKF) and the particle filter (PF) were used as model-based prognostics techniques based on the Bayesian tracking framework.

2. Related Work

In (Saha, Celaya, Wysocki, & Goebel, 2009a) a model-based prognostics approach for discrete IGBTs was presented. RUL prediction was accomplished by using a particle filter algorithm where the collector-emitter current leakage has been used as the primary precursor of failure. A prognostics approach for power MOSFETs was presented in (Saha, Celaya, Vashchenko, Mahiuddin, & Goebel, 2011). There, the threshold voltage was used as a precursor of failure; a particle filter was used in conjunction with an empirical degradation model. The latter was based on accelerated life test data.

Identification of parameters that indicate precursors to failure for discrete power MOSFETs and IGBTs has received considerable attention in the recent years. Several studies have focused on precursor of failure parameters for discrete IGBTs under thermal degradation due to power cycling overstress. In (Patil, Celaya, Das, Goebel, & Pecht, 2009), collector-emitter voltage was identified as a health indicator; in (Sonnenfeld, Goebel, & Celaya, 2008), the maximum peak of the collector-emitter ringing at the turn of the transient was identified as the degradation variable; in (Brown, Abbas, Ginart, Ali, Kalgren, & Vachtsevanos, 2010) the switching turn-off time was recognized as failure precursor; and switching ringing was used in (Ginart, Roemer, Kalgren, & Goebel, 2008) to characterize degradation. For discrete power MOSFETs, on-resistance was identified as a precursor of failure for the die-solder degradation failure mechanism (Celaya, Saxena, Wysocki, Saha, & Goebel, 2010a; Celaya, Patil, Saha, Wysocki, & Goebel, 2009). A shift in threshold voltage was named as failure precursor due to gate structure degradation fault mode (Celaya, Wysocki, Vashchenko, Saha, & Goebel, 2010b; Saha, et al., 2011).

There have been some efforts in the development of degradation models that are a function of the usage/aging time based on accelerated life test. For example, empirical degradation models for model-based prognostics were presented in (Saha, et al., 2009a) and (Saha, et al., 2011) for discrete IGBTs and power MOSFET respectively. Gate structure degradation modeling discrete power MOSFETs under ion impurities was presented in (Ginart, Ali, Celaya, Kalgren, Poll, & Roemer, 2010).

3. Background

3.1. Accelerated Aging Experiments

Accelerated aging approaches provide a number of opportunities for the development of physics-based prognostics models for electronic components and systems. In particular, they allow for the assessment of reliability in a considerably shorter amount of time than running long-term reliability tests. The development of prognostics algorithms face some of the same constrains as reliability engineering in that both need information about failure events of critical electronics systems. However, these data are rarely ever available. In addition, prognostics requires information about the degradation process leading to an irreversible failure; therefore, it is necessary to record *in-situ* measurements of key output variables and observable parameters in the accelerated aging process in order to develop and learn failure progression models.

Thermal cycling overstress leads to thermo-mechanical stresses in electronics due to mismatch of the coefficient of thermal expansion between different elements in the component's packaged structure. The accelerated aging applied to the devices presented in this work consisted of thermal overstress. Latch-up, thermal run-away, or failure to turn ON due to loss of gate control were considered as the failure condition. Thermal cycles were induced by power cycling the devices without the use of an external heat sink. The device case temperature was measured and directly used as control variable for the thermal cycling application. For power cycling, the applied gate voltage was a square wave signal with an amplitude of ~15V, a frequency of 1KHz and a duty cycle of 40%. The drain-source was biased at 4Vdc and a resistive load of 0.2Ω was used on the collector side output of the device. The aging system used for these experiments is described in detail in (Sonnenfeld, et al., 2008). The accelerated aging methodology used for these experiments was presented in detail in (Celaya, et al., 2010a).

Figure 1 shows an X-ray image and a scanning acoustic image of the device after degradation. It can be observed that the die-attach solder has migrated resulting in voids. This supports the observation that the thermal resistance from junction to case has increased during the stress time resulting in increase of the junction temperature and ON-resistance ($R_{DS(ON)}$). Figure 2 presents a plot of the measured $R_{DS(ON)}$ as a function of case temperature for several

consecutive aging tests on the same device. For each test run, the temperature of the device was increased from room temperature to a high temperature setting thus providing the opportunity to characterize $R_{DS(ON)}$ as a function of time at different degradation stages. It can be observed how this curve shifts as a function of aging time, which is indicative of increased junction temperature due to poor heat dissipation and hence degraded die-attach.

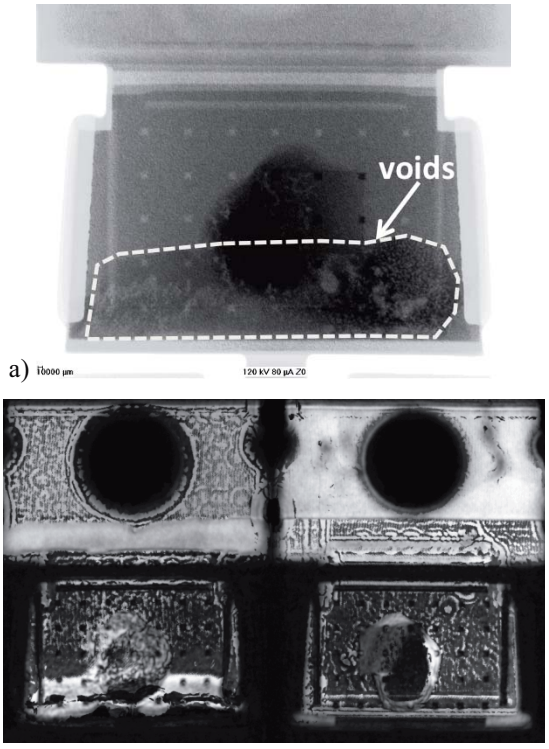

Figure 1. Failure analysis of a device after thermal overstress aging: a) X-ray microscopy of the degraded device and b) scanning acoustic microscopy of the degraded device.

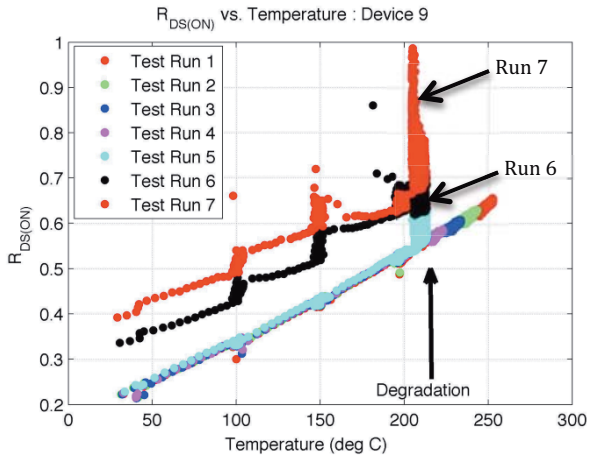

Figure 2. R_{DSON} degradation process due to die-attach damage.

Seven aging runs were performed in order to provide evidence of the underlying hypothesis that damage accumulates as a function of aging time and that damage rate is higher for aging under higher stress conditions like higher operating temperature. Please refer to (Celaya, et al., 2010a) for further details on the experiments.

3.2. Device Physics Modeling

In earlier work, a finite element model (FEM) was developed for a power MOSFET similar to the IRF520Npbf in order to simulate the physical phenomenon under thermal stresses. This work was originally presented in (Celaya, Saxena, Vashchenko, Saha, & Goebel, 2011b). I-V characteristics at different gate bias voltage (V_{gs}) were obtained while keeping the generic simulation parameters reasonably close to the tested MOSFETs. From the mixed-mode simulation of a single transistor model it was observed that the safe operation area (SOA) becomes limited at higher temperatures by critical voltages and currents that can be identified by the instability points in the simulation results. Please refer to (Celaya, et al., 2011b) for further details on the simulation setup and results.

The two-transistor model in figure 3 was developed to represent a device with partial die-attach degradation. The objective was to represent a degraded device of total area W_t, with two independent power MOSFET transistors with area W_1 and W_2 respectively and $W_t = W_1 + W_2$. The first transistor in the model represents the area of the device without die-attach damage and nominal thermal resistance from junction to case. The second transistor represents the area of the device with degraded die-attach and increased thermal resistance from junction to case. The second transistors runs by principle at higher temperature representative of hot spot formation on the device.

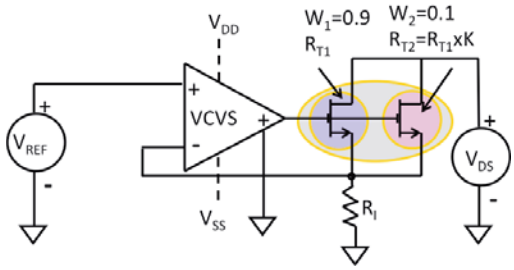

Figure 3. Two-transistor model circuit for mixed-mode simulation. Finite element models were used for each transistor.

The first transistor has original default parameters including the thermal resistance R_{T1} and area factor 90% while the second transistor depicts degradation due to electro-thermal stress represented by 10% of area with deviation of the thermal resistance coefficient scaled by the parameter K. As can be seen from the simulation results in figure 4, even a small deviation in the thermal resistance of the second transistor ($R_{T2}=K \text{x} R_{T1}$) results in significant reduction of the

critical voltage in auto bias conditions. Please refer to (Celaya, Saxena, Vashchenko, Saha, & Goebel 2011) for further details on the simulation setup and results.

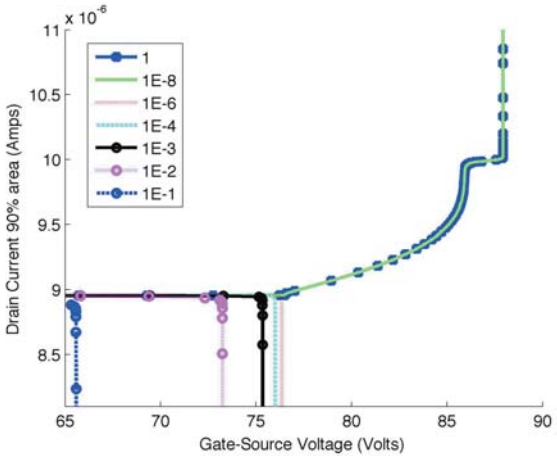

a)

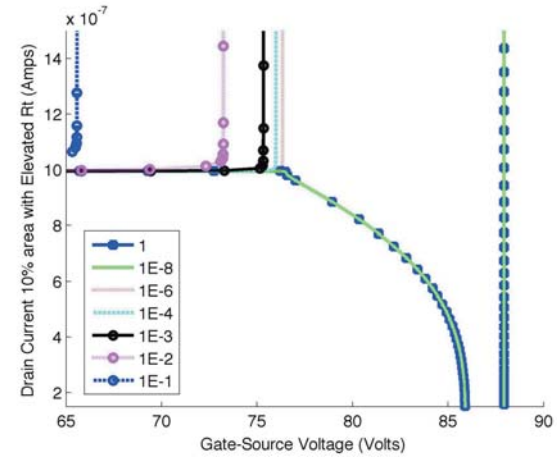

b)

Figure 4. Results of numerical analysis for different thermal resistance parameters K of the W_2=10% second transistor model region at 450K heat sink and R_{T2}=KxR_{T1}; a) nominal transistor with area W_1, b) degraded transistor with area W_2.

This model appears to be a good candidate for use in a physics-based degradation model. The model parameters K, W_1 and W_2 could be varied as the device degrades as a function of usage time, loading and environmental conditions. Parameter W_1 defines the area of the healthy transistors. The lower this area is, the larger is the degradation in the two-transistor model. Parameter K serves as a scaling factor for the thermal resistance of the degraded transistors. The larger this factor is, the larger is the degradation in the model. Similar to the empirical model used in this work and presented in later sections, the parameters of the two-transistor model should be estimated based on the actual fault progression dynamics.

3.3. Drain to source ON state resistance as a health state assessment parameter

In-situ measurements of the drain current (I_D) and the drain to source voltage (V_{DS}) are recorded as the device is in the aging regime and the power cycling is at 1 kHz square waveform. The ON-state resistance in this application was computed as the ratio of V_{DS} and I_D during the ON-state of the square waveform. As indicated in section 3.1, this parameter allows the observation of the die-attached degradation process and it is used in this study as a feature that reflects the state of health of the device. It is broadly understood that $R_{DS(ON)}$ increases as the junction temperature of the devices increases. In our accelerated aging setting, it is not possible to measure junction temperature directly, as a result, the increase in junction temperature is observed by monitoring the increase in $R_{DS(ON)}$ (Figure 2). Furthermore, junction temperature is also a function of the case temperature, which is also measured and recorded *in-situ*. Therefore, the measured $R_{DS(ON)}$ was normalized to eliminate the case temperature effects and reflect only changes due to degradation.

Due to manufacturing variability, the pristine condition $R_{DS(ON)}$ varies from device to device. In order to take this into account, the normalized $R_{DS(ON)}$ time series is shifted by applying a bias factor representing the pristine condition value. The resulting trajectory ($\Delta R_{DS(ON)}$) from pristine condition to failure represents the degradation process due to die-attach failure and represents the increase in $R_{DS(ON)}$ through the aging process.

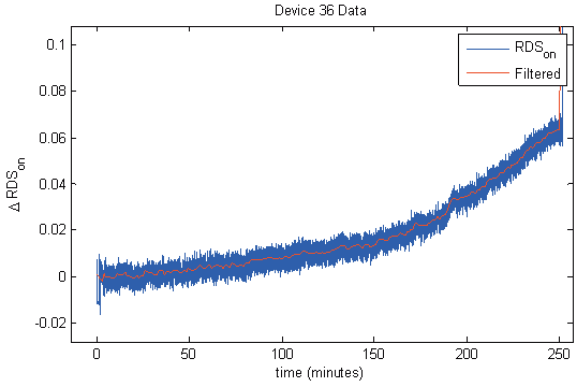

Figure 5. Normalized ON-state resistance ($\Delta R_{DS(ON)}$) and filtered trajectory for device #36.

As described earlier, these measurements are taken during the power cycle regime on the ON-state portion of the square switching signal. These measurements do not have a fixed sampling rate due to the nature of the implementation of the data acquisition system. On average, there is a transient response measurement every 400 nS. This consists of a snapshot of the transient response which includes one full square waveform cycle. The algorithms under consideration benefit from a uniform sampling in terms of ease of implementation and reduced complexity. Since the

complexity of GPR is $O(n^3)$, computational effort increases with number of data points and hence it is important to keep the number of training points low. A similar issue is also present on the EKF and PF. Therefore a resampling of the curve was carried out to have uniform sampling and a reduced sampling frequency on the failure precursor trajectory. In order to cope with these restrictions, the signals were filtered by computing the mean of every one minute long window (see Figure 5).

4. PROGNOSTICS ALGORITHMS

A prognostics algorithm in this application predicts the remaining useful life of a particular power MOSFET device at different points in time through the accelerated life of the device. Three algorithms are considered in this article, a data-driven algorithm based on the Gaussian process regression framework, and two model-based algorithms, the extended Kalman filter and the particle filter, which are based on the Bayesian estimation framework.

As indicated earlier, $\Delta R_{DS(ON)}$ is used in this study as a health indicator feature and as a precursor of failure. The prognostics problem is posed in the following way:

- A single feature is used to assess the health state of the device ($\Delta R_{DS(ON)}$).
- It is assumed that the die-attached failure mechanism is the only active degradation during the accelerated aging experiment.
- Furthermore, $\Delta R_{DS(ON)}$ accounts for the degradation progression from nominal condition through failure.
- Periodic measurements with fixed sampling rate are available for $\Delta R_{DS(ON)}$.
- A crisp failure threshold of 0.05 increase in $\Delta R_{DS(ON)}$ is used.
- The prognostics algorithm will make a prediction of the remaining useful life at time t_p, using all the measurements up to this point either to estimate the health state at time t_p in a regression framework or in a Bayesian state tracking framework.
- It is also assumed that the future load conditions do not vary significantly from past load conditions.

Six accelerated aging tests for power MOSFETs under thermal overstress were available. Figure 6 presents the $\Delta R_{DS(ON)}$ trajectories for the six cases. Cases #08, #09, #11, #12 and #14 are used for algorithm development purposes. They are used either as training data for regression models, as empirical data for degradation models or as data to quantify prior distributions' parameters of model and measurement noise and initial conditions. Case #36 is used to test the algorithms. The algorithms are developed and tested on the accelerated aging test timescale. In a real world operation, the timescale of the degradation process and therefore the RUL predictions will be considerably larger. It is hypothesized that even though the timescale will be larger, it remains constant through the degradation process and the developed algorithms and models would still apply under the slower degradation process. On the other hand, the algorithms under consideration have been used on several other prognostics applications. Here, by using accelerated aging data with actual device measurements and real sensors (no simulated behavior), we attempted to assess how such algorithms behave under these more realistic conditions.

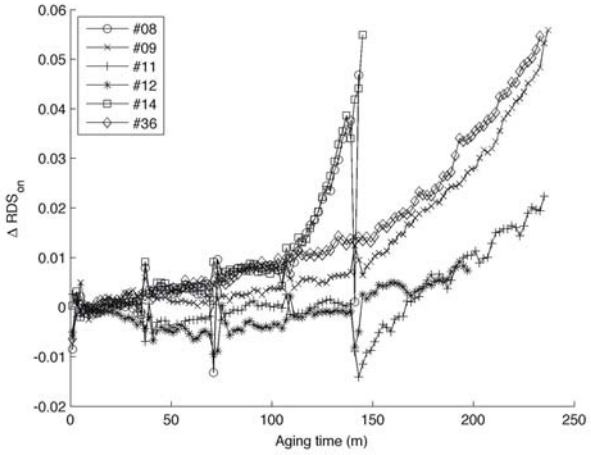

Figure 6: $\Delta R_{DS(ON)}$ trajectories for all MOSFETs, #36 is used to test algorithms and the rest are used for degradation model development and algorithm training (if required).

4.1. Degradation modeling

An empirical degradation model is suggested based on the degradation process observed on $\Delta R_{DS(ON)}$ for the five training devices. It can be seen that this process grows exponentially as a function of time and that the exponential behavior starts at different points in time for different devices. An empirical degradation model can be used to model the degradation process when a physics-based degradation model is not available. This methodology has been used for prognostics of electrolytic capacitors using a Kalman filter (Celaya, Kulkarni, Biswas, & Goebel, 2011a). There, the exponential degradation model was posed as a linear first order dynamic system in the form of a state-space model representing the dynamics of the degradation process. The proposed degradation model for the power MOSFET application is defined as

$$\Delta R_{DS(ON)} = \alpha(e^{\beta t} - 1), \qquad (1)$$

where t is time and α and β are model parameters that could be static or estimated on-line as part of the Bayesian tracking framework. This model structure is capable of representing the exponential behavior of the degradation process for the different devices (see Figure 6). It is clearly observed that the parameters of the model will be different for different devices. Therefore, the parameters α and β need to be estimated online in order to ensure accuracy. This

empirical degradation model is posed as a dynamic system as follows. Let $R = \Delta R_{DS(ON)}$, then

$$\frac{dR}{dt} = R\beta + \alpha\beta. \quad (2)$$

In this model, α and β are also state variables that change through time. Therefore, the model is a non-linear dynamic system and Bayesian tracking algorithms like the extended Kalman and particle filter are needed for on-line state estimation.

4.2. Gaussian process regression

Gaussian Process Regression (GPR) is a data-driven technique that can be used to estimate future fault degradation based on training data collected from measurement data. First, a prior distribution is assumed for the underlying process function that may be derived from domain knowledge (Goebel, Saha, & Saxena, 2008). Then this prior is tuned to fit available measurements which is used with the probabilistic function for regression over the training points (Rasmussen & Williams, 2006). The output is a mean function to describe the behavior and a covariance function to describe the uncertainty. These functions can then be used to predict a mean value and corresponding variance for a given future point of interest. The behavior of a dynamic process is captured in the covariance function chosen for the Gaussian process. The covariance structure also incorporates prior beliefs of the underlying system noise. A covariance function consists of various hyper-parameters that define its properties. Proper tuning of these hyper-parameters is key in the performance. While a user typically needs to specify the type of covariance function, the corresponding hyper-parameters can be learned from training data using a gradient based optimization (or other optimization) such as maximizing the marginal likelihood of the observed data with respect to hyper-parameters (Rasmussen & Williams, 2006).

4.3. Extended Kalman filter

Extended Kalman filter allows for the implementation of the Kalman filter algorithm for on-line estimation on non-linear dynamic systems (Meinhold & Singpurwalla, 1983; Welch & Bishop, 2006). This algorithm has been used in other applications for health state estimation and prognostics (Saha, Goebel, & Christophersen, 2009b). The extended Kalman filter general form is as follows.

$$x_k = f(x_{k-1}, u_{k-1}) + w_{k-1} \quad (3)$$
$$y_k = h(x_k) + v_k,$$

where f and h are non-linear equations, w_{k-1} is the model noise and v_k is the measurement noise. Noise is considered to be normally distributed with zero mean and known variance. For the prognostics implementation using the degradation model in equation (1) the state variable is defined as $x = \{R, \alpha, \beta\}$, therefore f is a vector valued function. Equation (2) gives the state transition equation for variable R; α and β are consider constant but they need to be estimated, therefore $\frac{d\alpha}{dt} = \frac{d\beta}{dt} = 0$ as part of the state transition function f. Measurements of R are available periodically but not for α and β. Therefore y_k will be a scalar representing the measured R at step k and h will be a scalar function defined as $h(x_k) = R$.

4.4. Particle filter

Particle filters (PFs) are based on Bayesian learning networks and are often used to track progression of system state in order to make estimations of remaining useful life (RUL. Bayesian techniques also provide a general rigorous framework for such dynamic state estimation problems. The core idea is to construct a probability density function (pdf) of the state based on all available information. In the Particle Filter (PF) approach (Arulampalam, Maskell, Gordon, & Clapp, 2002; Gordon, Salmond, & Smith, 1993) the pdf is approximated by a set of particles (points) representing sampled values from the unknown state space, and a set of associated weights denoting discrete probability masses. The particles are generated and recursively updated from a nonlinear process model that describes the evolution in time of the system under analysis, a measurement model, a set of available measurements and an a priori estimate of the state pdf. In other words, PF is a technique for implementing a recursive Bayesian filter using Monte Carlo (MC) simulations, and as such is known as a sequential MC (SMC) method.

Particle filter methods assume that the state equations can be modeled as a first order Markov process with the outputs being conditionally independent which can be written as:

$$x_k = f(x_{k-1}) + \omega_k$$
$$y_k = h(x_k) + \nu_k$$

where, k is the time index, x denotes the state, y is the output or measurements, and both ω and ν are samples from noise distributions. For this application, the PF framework was used to first track the degradation of $R_{DS(ON)}$ and then predict the remaining useful life of the power MOSFET based on whether the damage threshold has been reached by $R_{DS(ON)}$. The degradation model is presented in (1) and α and β are coefficients that are estimated initially by simple curve fitting for a few initial iterations. The PF uses the parameterized exponential growth model for $\Delta R_{DS(ON)}$, described above, for the propagation of the particles in time where the state vector is $\Delta R_{DS(ON)}$. The measurement vector comprises of the $\Delta R_{DS(ON)}$ parameters inferred from measured data. The values of α and β are learnt from regression on few initial inputs and are used as initial estimates for the filter.

5. REMAINING USEFIL LIFE PREDICTION RESULTS

This section presents the results of the three algorithms implemented. Device #36 was used to test the RUL predictions provided by the different algorithms. RUL predictions for device #36 are made at t_p: 140, 150, 160, 170, 180, 190, 195, 200, 205 and 210 minutes into aging. Subtracting the time when the prediction was made from the time when the predicted increase in resistance crosses the failure threshold gives the estimated remaining component life. As more data become available, the predictions are expected to become more accurate and more precise.

Figure 7 presents the state estimation results for $\Delta R_{DS(ON)}$ and the forecasting of $\Delta R_{DS(ON)}$ after measurements are no longer available. In this figure, measurements are available up to time t_p. They are used by all three algorithms to adjust the state estimation. The prediction step starts after t_p and time of failure t_{EOL}=228 hrs. A detail plot focusing around t_{EOL} is presented in Figure 8.

Analysis of the subplots from top to bottom shows how the prediction progresses as more data become available and the device gets closer to end of life. It also illustrates how prognostics is a series of periodic RUL predictions throughout the life of the device. The results as presented in Figure 7 and Figure 8 do not allow for a direct comparison among the three algorithms under consideration. Rather, it is to visually assess the estimation and prediction process. A quantitative assessment of the performance is required for direct comparison.

Figure 9 presents the α-λ performance metric for the three algorithms. This metric quantifies and visualizes the RUL prediction performance through time (Saxena, Celaya, Balaban, Goebel, Saha, Saha, & Schwabacher, 2008). The y-axis represents the estimated RUL at the time indicated in the x-axis. Ground truth RUL (*RUL**) information is used in this metric in order to assess the quality of the estimated RUL trajectories and it is identified by the 45° line in the plot. From this metric it was observed that the GPR approach is able to make predictions only at a considerably later time compared to the model-based approaches. This behavior is expected since the GPR method is data-driven and does not have the benefit of a model of the degradation process. Instead, the degradation process needs to start to get close to the elbow point of the exponential behavior in order for the prediction of RUL to become reasonably accurate. In general, the three approaches are all able to handle the RUL prediction process and predictions enter the α bound early in the life of the device. The RUL prediction results along with the prediction error are tabulated in Table 1.

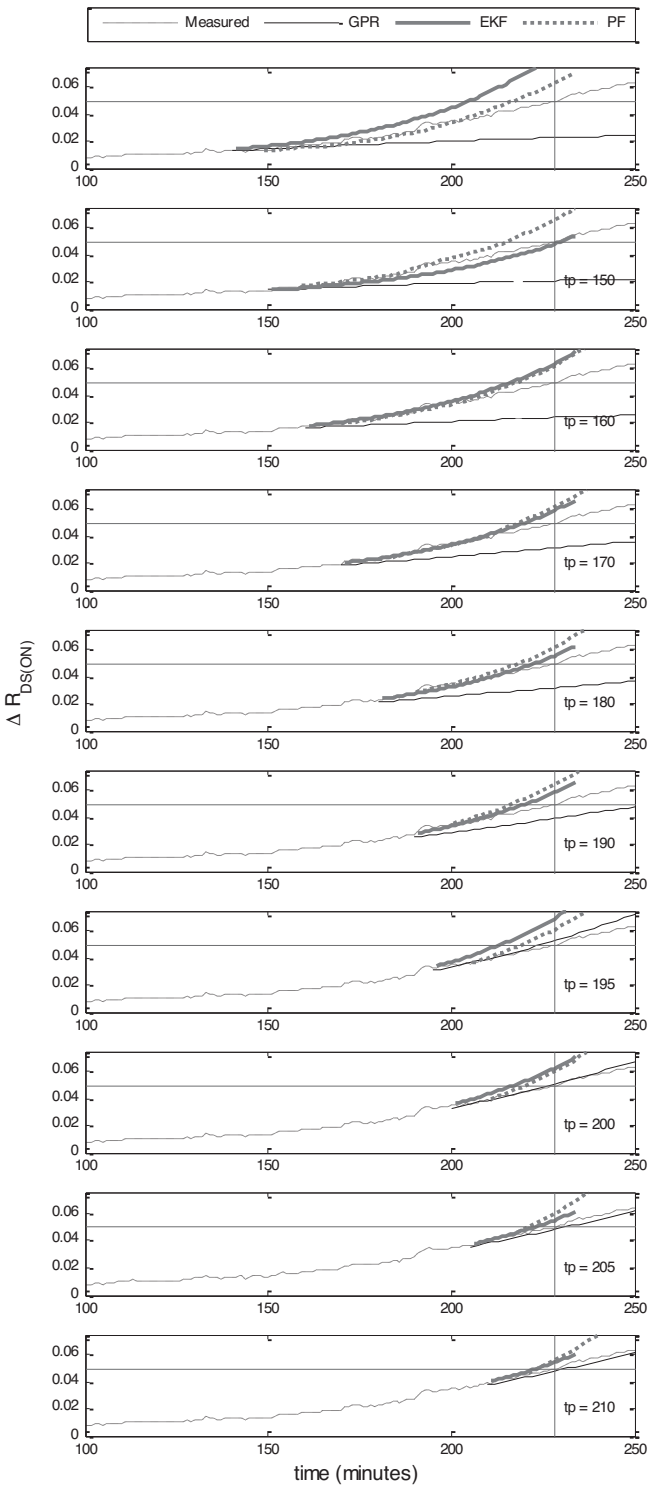

Figure 7: Health state ($\Delta R_{DS(ON)}$) tracking and forecasting for GPR, EKF and PF. Forecasting at t_p: 140, 150, 160, 170, 180, 190, 195, 200, 205 and 210 (min).

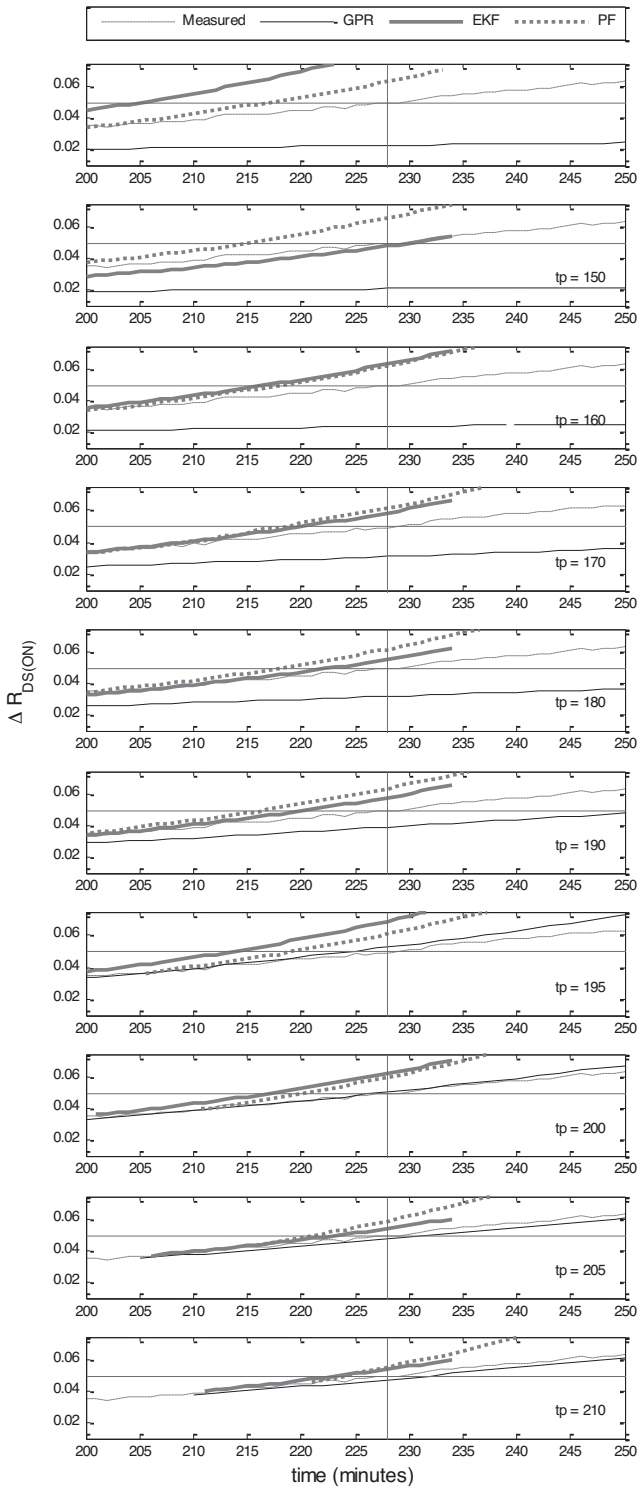

Figure 8: Detail of the health state ($\Delta R_{DS(ON)}$) tracking and forecasting for GPR, EKF and PF. Forecasting at t_p: 140, 150, 160, 170, 180, 190, 195, 200, 205 and 210 (min).

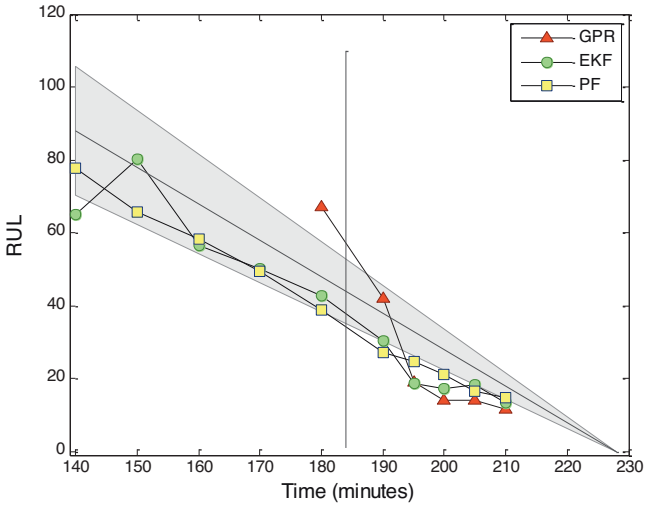

Figure 9: RUL prediction performance assessment for GPR, EKF and PF using the α-λ prognostics metric.

Table 1: RUL prediction results for GPR, EKF and PF at different t_p and t_{EOL}=228 hrs. RUL prediction error is between parentheses.

t_p	*RUL**	GPR	EKF	PF
140	88	N/A	64.98 (23.02)	77.65 (10.35)
150	78	N/A	80.22 (-2.22)	65.85 (12.15)
160	68	N/A	56.64 (11.36)	58.33 (9.67)
170	58	N/A	50.15 (7.85)	49.47 (8.53)
180	48	73.2 (-25.2)	42.75 (5.25)	38.68 (9.32)
190	38	33.4 (4.6)	30.35 (7.65)	27.14 (10.86)
195	33	17.6 (15.4)	18.57 (14.43)	24.76 (8.24)
200	28	14.6 (13.4)	17.24 (10.76)	21.09 (6.91)
205	23	13.8 (9.2)	18.28 (4.72)	16.66 (6.34)
210	18	11.8 (6.2)	13.46 (4.54)	14.68 (3.32)

6. CONCLUSION

The paper reports on a case study of employing data-driven and model-based techniques for the prediction of remaining life of power MOSFETs. Several strong assumptions were made that need to be challenged in order to make the proposed process practical for field use. For instance, the future operational conditions and loading of the device are

considered constant at the same magnitudes as the loads and conditions used during accelerated aging. In addition, the algorithm development is conducted using accelerated life test data. In real world implementation, the degradation process of the device would occur in a considerably larger time scale. Determining the relationship between signatures from accelerated aging and signatures from "natural" aging is a topic of future work.

The algorithms considered in this study have been used as prognostics algorithms in different applications and are regarded as suitable candidates for component level prognostics. This work attempts to further the validation of such algorithms by presenting them with real degradation data including measurements from real sensors, which include all the complications (noise, bias, etc.) that are regularly not captured on simulated degradation data.

The *in-situ* data available for empirical degradation model development could be used to assess the two-transistor model parameters on an on-line tracking framework. The two-transistor model has the added advantage of being suitable to be included along the dynamics of the subsystem or system level. For instance, if the device is part of a power supply, the two-transistor model could be used as part of the whole power supply transfer function, therefore generating a system-level physics-based model with degradation parameters linked to the die-attach degradation process.

ACKNOWLEDGEMENT

This work was funded by the NASA Aviation Safety Program, projects IVHM and SSAT.

NOMENCLATURE

RUL	remaining useful life
$R_{DS(ON)}$	ON-state drain to source resistance
SOA	safe operation area of the power MOSFET
K	scaling factor for thermal resistance on the two-transistor model
W_1	are of nominal transistor in the two-transistor model
W_2	area of degraded transistor in the two-transistor model
R_{T1}	junction to case thermal resistance of the nominal transistor in the two-transistor model
R_{T2}	junction to case thermal resistance of degraded transistor in the two-transistor model
$\Delta R_{DS(ON)}$	normalized deviation in ON-resistance from drain to source
t_p	time of RUL prediction
t_{EOL}	time of end of life (time of failure)
I_D	drain current
V_{DS}	drain to source voltage
RUL^*	ground truth for RUL

REFERENCES

Arulampalam, S., Maskell, S., Gordon, N. J., & Clapp, T. (2002). A tutorial on particle filters for on-line non-linear/non-Gaussian Bayesian tracking. *IEEE Transactions on Signal Processing, 50*(2), 174-188.

Brown, D., Abbas, M., Ginart, A., Ali, I., Kalgren, P., & Vachtsevanos, G. (2010). *Turn-off Time as a Precursor for Gate Bipolar Transistor Latch-up Faults in Electric Motor Drives.* Paper presented at the Annual Conference of the Prognostics and Health Management Society 2010.

Celaya, J., Kulkarni, C., Biswas, G., & Goebel, K. (2011a). *Towards Prognostics of Electrolytic Capacitors.* Paper presented at the AIAA Infotech@Aerospace, St. Louis, MO.

Celaya, J., Saxena, A., Wysocki, P., Saha, S., & Goebel, K. (2010a). *Towards Prognostics of Power MOSFETs: Accelerated Aging and Precursors of Failure.* Paper presented at the Annual Conference of the Prognostics and Health Management Society 2010.

Celaya, J. R., Patil, N., Saha, S., Wysocki, P., & Goebel, K. (2009). *Towards Accelerated Aging Methodologies and Health Management of Power MOSFETs (Technical Brief).* Paper presented at the Annual Conference of the Prognostics and Health Management Society 2009.

Celaya, J. R., Saxena, A., Vashchenko, V., Saha, S., & Goebel, K. (2011b). *Prognostics of Power MOSFET*. Paper presented at the 23nd International Symposium on Power Semiconductor Devices & IC's (ISPSD), San Diego, CA.

Celaya, J. R., Wysocki, P., Vashchenko, V., Saha, S., & Goebel, K. (2010b). *Accelerated aging system for prognostics of power semiconductor devices.* Paper presented at the 2010 IEEE AUTOTESTCON.

Ginart, A., Roemer, M., Kalgren, P., & Goebel, K. (2008). *Modeling Aging Effects of IGBTs in Power Drives by Ringing Characterization.* Paper presented at the IEEE International Conference on Prognostics and Health Management.

Ginart, A. E., Ali, I. N., Celaya, J. R., Kalgren, P. W., Poll, S. D., & Roemer, M. J. (2010). *Modeling SiO2 Ion Impurities Aging in Insulated Gate Power Devices Under Temperature and Voltage Stress.* Paper presented at the Annual Conference of the Prognostics and Health Management Society 2010.

Goebel, K., Saha, B., & Saxena, A. (2008). *A Comparison of Three Data-Driven Techniques for Prognostics*. Paper presented at the Proceedings of the 62nd Meeting of the Society For Machinery Failure Prevention Technology (MFPT).

Gordon, N. J., Salmond, D. J., & Smith, A. F. M. (1993). Novel Approach to Nonlinear/Non-Gaussian

Bayesian State Estimation. *IEE Proceedings Radar and Signal Processing, 140*(2), 107-113.

Meinhold, R. J., & Singpurwalla, N. D. (1983). Understanding the Kalman Filter. *The American Statistician, 37*(2), 123-127.

Patil, N., Celaya, J., Das, D., Goebel, K., & Pecht, M. (2009). Precursor Parameter Identification for Insulated Gate Bipolar Transistor (IGBT) Prognostics. *IEEE Transactions on Reliability, 58*(2), 276.

Rasmussen, C. E., & Williams, C. K. I. (2006). *Gaussian Processes for Machine Learning*.

Saha, B., Celaya, J. R., Wysocki, P. F., & Goebel, K. F. (2009a). *Towards prognostics for electronics components*. Paper presented at the Aerospace conference, 2009 IEEE.

Saha, B., Goebel, K., & Christophersen, J. (2009b). Comparison of prognostic algorithms for estimating remaining useful life of batteries. *Transactions of the Institute of Measurement and Control, 31*(3-4), 293-308. doi: 10.1177/0142331208092030

Saha, S., Celaya, J. R., Vashchenko, V., Mahiuddin, S., & Goebel, K. F. (2011). *Accelerated Aging with Electrical Overstress and Prognostics for Power MOSFETs.* Paper presented at the IEEE EnergyTech 2011.

Saxena, A., Celaya, J., Balaban, E., Goebel, K., Saha, B., Saha, S., & Schwabacher, M. (2008, 6-9 Oct. 2008). *Metrics for evaluating performance of prognostic techniques.* Paper presented at the Prognostics and Health Management, 2008. PHM 2008. International Conference on.

Sonnenfeld, G., Goebel, K., & Celaya, J. R. (2008). *An agile accelerated aging, characterization and scenario simulation system for gate controlled power transistors.* Paper presented at the IEEE AUTOTESTCON 2008.

Welch, G., & Bishop, G. (2006). An Introduction to the Kalman Filter (TR 95-041): Department of Computer Science, University of North Carolina at Chapel Hill.

BIOGRAPHIES

José R. Celaya is a research scientist with SGT Inc. at the Prognostics Center of Excellence, NASA Ames Research Center. He received a Ph.D. degree in Decision Sciences and Engineering Systems in 2008, a M. E. degree in Operations Research and Statistics in 2008, a M. S. degree in Electrical Engineering in 2003, all from Rensselaer Polytechnic Institute, Troy New York; and a B. S. in Cybernetics Engineering in 2001 from CETYS University, México.

Abhinav Saxena is a Research Scientist with SGT Inc. at the Prognostics Center of Excellence NASA Ames Research Center, Moffett Field CA. His research focus lies in developing and evaluating prognostic algorithms for engineering systems using soft computing techniques. He is a PhD in Electrical and Computer Engineering from Georgia Institute of Technology, Atlanta. He earned his B.Tech in 2001 from Indian Institute of Technology (IIT) Delhi, and Masters Degree in 2003 from Georgia Tech. Abhinav has been a GM manufacturing scholar and is also a member of IEEE, AAAI and ASME.

Sankalita Saha is a research scientist with Mission Critical Technologies at the Prognostics Center of Excellence, NASA Ames Research Center. She received the M.S. and PhD. degrees in Electrical Engineering from University of Maryland, College Park in 2007. Prior to that she obtained her B.Tech (Bachelor of Technology) degree in Electronics and Electrical Communications Engineering from the Indian Institute of Technology, Kharagpur in 2002.

Kai Goebel received the degree of Diplom-Ingenieur from the Technische Universitt Mnchen, Germany in 1990. He received the M.S. and Ph.D. from the University of California at Berkeley in 1993 and 1996, respectively. Dr. Goebel is a senior scientist at NASA Ames Research Center where he leads the Diagnostics and Prognostics groups in the Intelligent Systems division. In addition, he directs the Prognostics Center of Excellence and he is the Associate Principal Investigator for Prognostics of NASA's Integrated Vehicle Health Management Program. He worked at General Electric's Corporate Research Center in Niskayuna, NY from 1997 to 2006 as a senior research scientist. He has carried out applied research in the areas of artificial intelligence, soft computing, and information fusion. His research interest lies in advancing these techniques for real time monitoring, diagnostics, and prognostics. He holds 15 patents and has published more than 200 papers in the area of systems health management.